OXFORD

Carcinogenesis, 2016, Vol. 37, No. 12, 1190–1198

doi:10.1093/carcin/bgw101
Advance Access publication September 21, 2016
Original Manuscript

ORIGINAL MANUSCRIPT

Novel *Helicobacter* species *H.japonicum* isolated from laboratory mice from Japan induces typhlocolitis and lower bowel carcinoma in C57BL/129 IL10$^{-/-}$ mice

Zeli Shen[1], Yan Feng[1], Sureshkumar Muthupalani[1], Alexander Sheh[1], Lenzie E.Cheaney[1], Christian A.Kaufman[1], Guanyu Gong[2], Bruce J.Paster[3] and James G.Fox[1,2,*]

[1]Division of Comparative Medicine, [2]Department of Biological Engineering, Massachusetts Institute of Technology, Cambridge, MA 02139, USA and [3]The Forsyth Institute, Cambridge, MA 02139, USA

*To whom correspondence should be addressed. Tel: +1 617 253 1757; Fax: +1 617 258-5708; Email: jgfox@mit.edu

Abstract

A novel *Helicobacter* species *Helicobacter japonicum* was isolated from the stomach and intestines of clinically normal mice received from three institutes from Japan. The novel *Helicobacter* sp. was microaerobic, grew at 37°C and 42°C, was catalase and oxidase positive, but urease negative. It is most closely related to the 16S rRNA gene of *H.muridarum* (98.6%); to the 23S rRNA gene of *H.hepaticus* (97.9%); to the *hsp60* gene of *H.typhlonius* (87%). The novel *Helicobacter* sp. has *in vitro* cytolethal distending toxin (CDT) activity; its *cdt*B gene sequence has 83.8% identity with that of *H.hepaticus*. The whole genome sequence of *H.japonicum* MIT 01-6451 has a 2.06-Mb genome length with a 37.5% G + C content. When the organism was inoculated into C57BL/129 IL10$^{-/-}$ mice, it was cultured from the stomach, colon and cecum of infected mice at 6 and 10 weeks post-infection. The cecum had the highest *H.japonicum* colonization levels by quantitative PCR. The histopathology of the lower bowel was characterized by moderate to severe inflammation, mild edema, epithelial defects, mild to severe hyperplasia, dysplasia and carcinoma. Inflammatory cytokines IFNγ, TNFα and IL17a, as well as iNOS were significantly upregulated in the cecal tissue of infected mice. These results demonstrate that the novel *H.japonicum* can induce inflammatory bowel disease and carcinoma in IL10$^{-/-}$ mice and highlights the importance of identifying novel *Helicobacter* spp. especially when they are introduced from outside mouse colonies from different geographic locations.

Introduction

Helicobacter species infections have been reported worldwide. *Helicobacter pylori*, the type species of gastric helicobacter has been linked to development of two forms of gastric cancer, gastric adenocarcinoma and gastric mucosa-associated lymphoma, and is also linked to the development of peptic ulcers. Select enterohepatic *Helicobacter* species (EHS) such as *Helicobacter winghamensis*, *H.pullorum*, *H.canadensis*, *H.cinaedi*, *H.trogontum*, *H.bilis* and *H.fennelliae* are associated with gastroenteritis, bacteremia, cellulitis and inflammatory bowel disease (IBD) in humans. Naturally acquired *Helicobacter* spp. infections have been isolated most commonly in laboratory rodents. Some of those EHS species have been linked to disease development in susceptible hosts. *Helicobacter hepaticus* induces hepatitis and hepatocellular carcinoma in the liver in A/JCr mice; causes chronic intestinal inflammation in A/JCr, germfree Swiss Webster mice and immunodeficient mice; *H.hepaticus* also leads to IBD, associated colon cancer in immune-dysregulated mice (1). *Helicobacter bilis* is associated with hepatitis in aged inbred and outbred mice; caused IBD and colon cancer in severe combined immunodeficient mice multiple-drug resistance-deficient mice, and WASP-deficient mice and increases the susceptibility for gall stone formation in C57L/J mice (2–6). Several novel

Received: April 22, 2016; **Revised:** August 29, 2016; **Accepted:** September 12, 2016

Abbreviations

CDT	cytolethal distending toxin
DSB	double-strand break
EHS	enterohepatic *Helicobacter* species
GIN	gastrointestinal intraepithelial neoplasia
IBD	inflammatory bowel disease
p.i	post-infection

EHS have been reported in recent years. Most EHS infections in immunocompetent mice are subclinical, but they can significantly affect the results of experiments in infected laboratory mice (7–9). Exclusion of EHS from mouse colonies will reduce the risk of compromising research results and will decrease clinical disease in many transgenic mouse strains. Recognition of their importance has prompted screening for EHS in mouse health monitoring protocols in many research institutes.

In our previous study, we isolated a novel *Helicobacter* sp. (MIT 01-6451) from mice from Japan during a survey of mice from commercial and academic institutions in Asian, Europe and Northern America (10). Subsequently, this species was reported to colonize a high prevalence of mice used in biomedical research in Japan (11,12). In this study, additional strains of this mouse *Helicobacter* spp. having the same 16S rRNA gene sequences as MIT 01-6451, were isolated from mice shipped to MIT from three institutes from Japan, and the phenotypic and phylogenetic characteristics of this novel *Helicobacter* sp. were evaluated. Using C57BL/6 IL10$^{-/-}$ mice, we also determined whether this novel species *H.japonicum* (MIT 01-6451) induced IBD and lower bowel carcinoma in C57BL/129 IL10$^{-/-}$ mice.

Material and methods

Animals

The novel *Helicobacter* species was isolated from six mice, obtained from three different research institutes in Japan, shipped to MIT principal investigators for research purposes. All the mice were immunocompetent and clinically normal (three Dppa2-MerCreMerPEST C57BLD2F2 mice; two WGA FVB/N transgenic mice and one C57BL/129-Lefty1tm1Hmd mouse) (13–15). After using these mice for rederivation through embryo transfer to establish specific pathogen free mice for introduction into our AAALAC research mouse facilities, the mice were euthanized with CO_2. The stomach, colon, cecum and feces were collected from each mouse for helicobacter culture and PCR.

Bacterial isolation

Tissue and fecal samples previously frozen at –80°C in 20% glycerol in Brucella broth were homogenized and the aliquots of each slurry was placed on cefoperazone, vancomycin and amphotericin B (CVA) plates or passed through a 0.65-μm syringe filter onto a trypticase soy agar plate with 5% sheep blood (Remel Laboratories, Lenexus, KS). The plates were incubated at 25°C, 37°C and 42°C under microaerobic conditions in the vented jar containing N_2, H_2 and CO_2 (80:10:10); and were checked every 2–3 days for bacterial growth for 3 weeks. Suspected bacterial growth was identified as *Helicobacter* spp. on the basis of colony morphology, phase microscopy and Gram staining. Detailed biochemical characterization analysis was performed on five individual isolates (including MIT 01-6451) using RapID™ NH System (Remel Laboratories, Lenexus, KS) and API Campy kit (BioMérieux, Boston, MA). Biochemical characterization of urease, catalase and oxidase productions, sensitivity to nalidixic acid and cephalothin; as well as the growth in the presence of 1% glycine were conducted as previously described by our laboratory. A disc assay was used for indoxyl acetate hydrolysis (16).

Electron microscopy

Helicobacter japonicum MIT 01-6451 was examined by electron microscopy. Cells grown on blood agar plates were centrifuged and gently suspended in 10 mM Tris–HCl buffer (pH 7.4) at a concentration of about 10^8 cells per ml. Samples were negatively stained with 1% (wt/vol) phosphotungstic acid (pH 6.5) for 20–30 s. The specimens were examined with a JEOL model JEM-1200EX transmission electron microscope operating at 100 kV.

Genomic DNA extraction and 16S rRNA sequencing

The High Pure PCR template preparation kit (Roche Molecular Biochemicals, Indianapolis, IN) was used for bacteria and mouse tissue DNA extraction according to the manufacturer's protocols. The full length of 16S rRNA of six strains were amplified with primer 9F (5′ GAG TTT GAT YCT GGC TCA G) and 1541R (5′ AAG GAG GTG WTC CAR CC). Sequence alignments and phylogenetic analysis of 16S rRNA, 23S rRNA of MIT 01-6451, obtained from whole genome sequence, were performed using the Geneious bioinformatics software package (Geneious v7.1.7, Biomatters Ltd., Auckland, New Zealand).

Whole genome sequencing of strain MIT 01-6451

Genomic DNA was sequenced using Illumina MiSeq sequencing technology as described previously (17). The 250-bp paired-end sequencing reads generated by MiSeq were assembled into contigs using Velvet (18). Sequences were annotated using the NCBI Prokaryotic Genomes Automatic Annotation Pipeline (19).

Experimental infection of C57BL/129 IL 10$^{-/-}$ mice

Forty C57BL/129 IL 10$^{-/-}$ (B6.129P2-IL-10*tm1Cgn*) mice from a breeding colony maintained at the Massachusetts Institute of Technology (MIT), with equal numbers of male and female mice aged 6–8-week-old were used in the study. Twenty C57BL mice (10 males, 10 females) were purchased from The Jackson Laboratory (Bar Harbor, ME). Mice were maintained free of known murine viral pathogens, *Salmonella* spp., *Citrobacter rodentium*, ecto- and endoparasites and known *Helicobacter* spp. and housed in an AAALAC accredited facility under barrier conditions. Animals were housed in microisolater, solid-bottomed polycarbonate cages on hardwood bedding, fed a commercial pelleted diet and administered water ad libitum. The protocol was approved by the Committee on Animal Care of the Massachusetts Institute of Technology.

Helicobacter japonicum MIT 01-6451 was grown under microaerobic condition at 37°C on 5% sheep blood agar plate for 2–3 days. Bacteria were collected using a cotton swab and resuspended in Brucella broth with 20% glycerol and adjusted the bacteria concentration to 1 OD_{600}/ml. Mice received 0.2 ml of fresh inoculum by gastric gavage every other day for three doses or controls were sham-dosed with broth only. Twenty C57BL//129 IL10$^{-/-}$ mice were infected with *H.japonicum*; 20 mice were sham dosed as controls. Ten C57BL/6 mice were infected with *H.japonicum* MIT 01-6451, and another 10 mice served as controls. These mice were necropsied at 6 weeks post-infection (p.i). All groups were comprised of equal numbers of males and females. Colonization with *Helicobacter* sp. was confirmed 2 weeks post-inoculation by PCR analysis of feces using *Helicobacter* genus specific primers (20). C57BL IL10$^{-/-}$ mice were necropsied at 6 and 10 weeks p.i, and feces were collected followed by liver, stomach, cecum and colon for culture, quantitative PCR, RNA isolation and histology.

Histological evaluation

Formalin-fixed tissues were routinely processed, embedded in paraffin, cut at 4 μm and stained with hematoxylin and eosin (H&E). Large bowel lesions were scored on the basis of size and frequency of hyperplastic and inflammatory lesions on a scale of 0–4 with ascending severity (0, none; 1, minimal; 2, mild; 3, moderate and 4, severe). Epithelial dysplasia and neoplasia were graded using a scale of 0–4: 0, normal; 1, mild dysplastic changes; 2, moderate to severe dysplasia; 3, gastrointestinal intraepithelial neoplasia (GIN) and 4, invasive carcinoma as previously described (21,22).

Quantitative PCR for *H.japonicum* colonization levels in liver, cecum, colon and stomach tissues of infected mice

Relative concentrations of *Helicobacter* spp. DNA in infected mice were determined by real-time quantitative PCR using the ABI Prism Taqman 7500 Fast real-time PCR system (PE Biosystems, Foster City, CA). DNA was extracted from tissues using a High Pure PCR Template Preparation Kit

(Roche Molecular Biochemicals, Indianapolis, IN) following the manufacturer protocol. *Helicobacter* genus specific primers were used, with forward primer QHE-F 5′ ACC AAG GC(A/T) ATG ACG GGT ATC-3′) (positions 406–426), and reverse primer QHE-R′-CGG AGT TAG CCG GTG CTT ATT-3′ (positions 606–626), fluorescently labeled *Helicobacter* spp. probe (FAM-AAC CTT CAT CCT CCA CGC GGC-TAMRA) (positions 535–555) (23). Duplicate PCR reactions contained the following in 20 µl volumes: 5 µl of template DNA; 10 µl Universal Master Mix; 200 nM of each primer and 100 nM of probe. Thermocycling was performed at 95°C for 20 s, and then 40 repeats of 95°C for 3 s and 60°C for 30 s. Samples were also probed with 18S rRNA-based primers for quantifying host DNA (Applied Biosystems) as previously described (24,25).

Cytokine mRNA expression profiles in the lower bowel of IL10$^{-/-}$ mice and wildtype mice

RNA was extracted from ~25 mg of mouse tissue at the ileo-cecal colic junction using Trizol reagent (Invitrogen, Carlsbad, CA). Total RNA (2 µg) was converted into cDNA using a high capacity cDNA Archive kit following the manufacturer protocol (Applied Biosystems). cDNA levels for TNF-α, IFN-γ, iNOS, IL4, IL6, IL23a and IL17a mRNA were measured by quantitative PCR using commercial primers and probes for each cytokine. Briefly, duplicate 20 µl reactions contained 5 µl of cDNA, 1 µl of a commercial 20× primer-probe solution, 10 µl of 2× master mix (all Applied Biosystems) and 4 µl of double-distilled H_2O. Relative expression of mRNA from infected and control mice was calculated using the comparative C_T method with RNA input standardized between samples by expression levels of the endogenous reference gene, GAPDH. Results from duplicate samples were plotted as fold changes between tissues from infected and uninfected control mice.

Fluorescence *in situ* hybridization

Probes based on 16S rRNA gene of *Helicobacter* sp. genus were used to detect the novel *Helicobacter* sp. in the paraffin embedded intestinal tissues (26). Briefly, paraffin sections of ceca or colons from *H.japonicum* infected IL10$^{-/-}$ mice were deparaffinized and rehydrated. A combination of two probes, HEL274 and HEL717, labeled with Cy3 were used to increase the intensity of the signals (Integrated DNA Technologies, Coralville, IA) (26). Hybridization buffer (0.9 M NaCl, 20 mM Tris–HCl, 0.01% SDS, 30% formamide) with 5 ng/ml of each probe was preheated for 10 min at 74.5 °C; 80 ul of this solution was added to each slide. Slides were covered in parafilm, and placed in a dark humidification chamber overnight at 48°C. After incubation, slides were rinsed in double-distilled water and serially washed in pre-warmed rinsing buffers for 15 min each (Buffer 1: 0.9 M NaCl, 20 mM Tris–HCl, 0.01% SDS; Buffer 2: 0.9 M NaCl, 20 mM Tris–HCl). Slides were air-dried, mounted in Vectashield with DAPI (Vector Laboratories, Burlingame, CA), and examined under a Zeiss Axioskop 2 fluorescent microscope. Tissues were considered positive for *Helicobacter* sp. if fluorescent spiral organisms were observed using a Rhod filter.

Immunofluorescence staining of gamma H2AX and Ki-67

Formalin fixed paraffin embedded sections of mouse cecal tissue were deparaffinized with xylene and then rinsed sequentially with 100, 90, 70 ethanol and water. Antigen retrieval was performed using Dako target retrieval solution (modified citrate buffer) at 95°C for 20 min. The tissue sections were blocked using 3% bovine serum albumin in 1× phosphate-buffered saline 0.3% Triton at 4°C overnight. The primary antibody of gamma H2AX (Millipore, Billerica, MA) and Ki-67 antibody (rat anti-mouse Ki-67, Dako) were diluted 1/100 and incubated with tissue at 4°C for 3 h. The tissue section was then washed and labeled with secondary antibody Alexa Fluor-568 in 1/500 for H2AX; Alexa Fluor-488 in 1/500 for Ki-67 (Invitrogen. Grand Island, NY) and counter-stained with DAPI. Images were obtained using Image Pro-Plus (7.2 version, Media Cybematics, Silver Spring, MD) and QIClick digital CCD camera (Qimaging, Surrey, BC, Canada) mounted on a Zeiss Axioskop 2 plus microscope.

Results

Characterization of *H.japonicum*

Eight mice received from three different institutes in Japan were screened for *Helicobacter* spp. upon arrival at MIT. After incubation under microaerobic condition, *Helicobacter* spp.-like organisms were isolated from cecum and feces of 6 mice, and the stomach of one of these mice. Bacteria grew on the agar surface after 3–7 days of initial plating, appeared as a thin, spreading film and did not form single colonies. The bacteria grew at 37°C and 42°C but not 25°C. Gram staining revealed the isolates were gram negative with a curved shape. All the isolates were positive for catalase and oxidase. The isolates were negative for urease, alkaline phosphatase, indoxyl acetate and nitrate reduction. They did not grow on 1% glycine plates and were resistant to nalidixic acid and cephalothin (Table 1.)

Electron microscopy

By transmission electron microscopic examination, the bacteria were slender slightly curved rods, 0.3–0.4 um in diameter and length about 2–3 µm, with a single sheathed polar flagellum and occasionally were noted to have bipolar flagella (Supplementary Figure 1, available at *Carcinogenesis* Online).

Phylogenetic analysis of 16S rRNA and 23S rRNA gene analysis

Six strains of helicobacter isolates were subjected to 16S rRNA sequence analysis. The novel species from the six mice had the same 16S rRNA gene which clustered in the phylogenetic tree near *H.muridarum* and *H.typhlonius*, with identities of 98.6% to *H.muridarum* and 98% with *H.typhlonius*. (Figure 1A) The 23S rRNA gene sequence was obtained for strain MIT01-6451 by analysis of *H.japonicum* whole genome sequence, which was closely related to *H.typhlonius* with 98% identity. The degree of identity of 23S rRNA gene to *H.hepaticus* and *H.muridarum* was 97.9 and 97.8%, respectively (Figure 1B).

Table 1. Biochemical tests of *H.japonicum*

Species	42°C	25°C	1% L-glycine	Catalase	Oxidase	Urease	PO4	NO3	IAH	NA	CE
'*H.japonicum*' *n* = 5	+	—	—	+	+	—	—	—	—	R	R
H.hepaticus	—	—	+	+	+	+	—	+	+	R	R
H.rodentium	+	—	+	+	+	—	—	+	—	R	R
H.muridarum	—	—	—	+	+	+	+	-	+	R	R
H.bilis	+	—	+	+	+	+	—	—	—	R	R
H.mastomyrinus	+	—	+	+	+	—	—	—	—	R	R
H.typhlonius	+	—	+	+	+	—	—	—	—	R	R

Five strains of novel *Helicobacter* sp. were tested.
IAH, indoxyl acetate hydrolysis; NA, nalidixic acid; NO3, nitrate reduction; PO4, alkaline phosphatase hydrolysis.

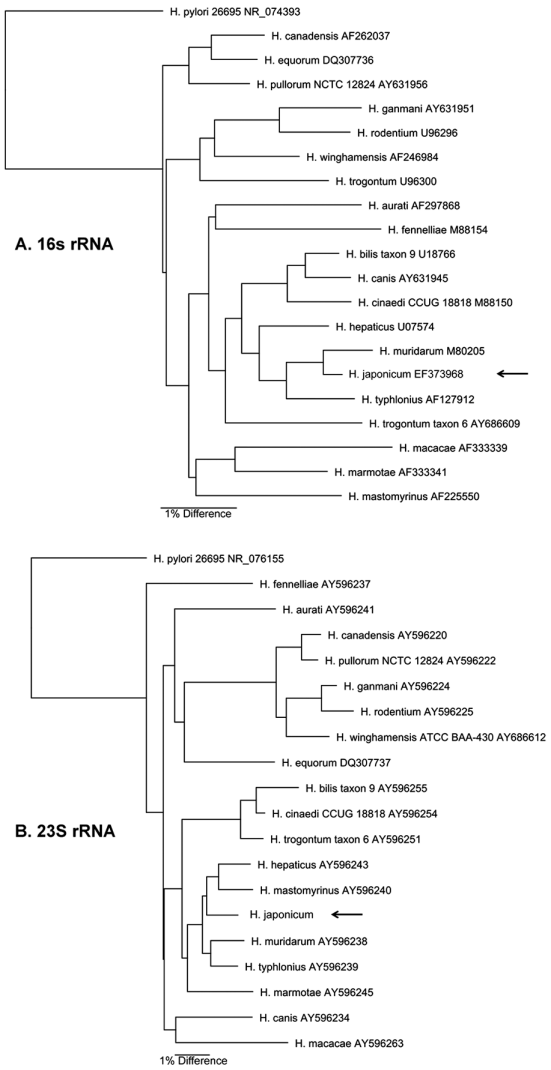

Figure 1. Phylogenic tree constructed based on the sequence similarity values.

Draft genome sequence of *H.japonicum*

Helicobacter japonicum MIT 01-6451 has a 37.5% GC content. Velvet assembly of 48 contigs greater than 250 bp in length revealed an estimated genome length of 2 Mb with 2064 genes was annotated using PGAP (27). In evaluating the presence of known *Helicobacter* spp. virulence determinants in MIT 01-6451, we found that cytolethal distending toxin (CDT) A, B and C units were present in this species. The *cdt*B gene from *H.hepaticus* ATCC 51449 and *H.japonicum* MIT 01-6451were aligned. Both genes were 822 bp long. There was 83.8% pairwise identity between the two species. The components of the type VI secretion systems (hcp, vasD and vgrG) associated with pathogenicity (28) were also found in this strain. However, gamma-glutamyl-transpeptidase (ggt) and Type IV secretion components were absent. The draft genome of MIT 01-6451 was submitted to Genbank under accession number JRMQ00000000 (27). The genes for *hsp60*, *rpoB* and *cdtB* of MIT 01-6451 from whole genome analysis were compared to other closely related *Helicobacter* spp. (Supplementary Table 1, available at *Carcinogenesis* Online).

Helicobacter japonicum MIT 01-6451 colonized the stomach, colon and cecum of C57BL/129 IL10$^{-/-}$ mice

To investigate the pathogenic potential of *H.japonicum* in animals, IL10$^{-/-}$ male and female mice were infected with MIT 01-6451or served as sham controls. Mice were necropsied at 6 and 10 weeks post-infection (p.i.). All sham-dosed mice remained *Helicobacter* sp. free as assessed by helicobacter-specific PCR. All the infected mice were colonized with *H.japonicum* in the cecum and colon at both time points by qPCR analysis. The cecum had the highest colonization levels. There was no difference in the colonization levels between 6 and 10 weeks p.i. Helicobacter DNA was also detected in 70% of the stomach samples at 6 weeks p.i and 56% of the stomach samples 10 weeks p.i; at much lower levels (Figure 2). All the liver samples were negative for helicobacter by qPCR and nested PCR with two sets of helicobacter genus specific primers (29). *Helicobacter japonicum* was also re-isolated from 4/4 cecum samples, 4/4 of colon samples and one of four stomach samples and confirmed to be identical to the strain 01-6451 by 16S rRNA sequencing (Supplementary Table 2, available at *Carcinogenesis* Online). Fluorescence *in situ* hybridization staining with helicobacter genus specific probes on the cecum tissue sections depicted red fluorescence labeled bacteria in the lumen and crypts of the intestines of infected mice (Supplementary Figure 2, available at *Carcinogenesis* Online). In C57BL/6 mice, *Helicobacter* colonization levels in the cecum of infected mice were significantly higher when compared with the colonization levels in the cecum of IL10$^{-/-}$ mice (See Supplementary Figure 6, available at *Carcinogenesis* Online). Male C57BL mice had higher *Helicobacter japonicum* colonization levels than female C57BL mice (data not shown).

Helicobacter japonicum MIT 01-6451 induced typhlocolitis and lower bowel carcinoma in IL10$^{-/-}$ mice

There was no significant body weight changes at 6 weeks p.i, but at 10 weeks p.i, the infected mice had significantly less body weight when compared with controls ($p < 0.01$) (Supplementary Figure 3, available at *Carcinogenesis* Online). The infected mice were less active and slightly hunched. All the infected mice developed typhlocolitis at 6 weeks p.i. The typhlocolitis index in the colon and cecum of infected mice were significantly higher than that of control mice ($P < 0.01$). The ileo-cecal colic junction had more severe lesions than those observed in the transverse and lower colon. The cumulative lesions in the ileo-cecal colic tissues at 6 weeks p.i were more severe than lesions at 10 weeks p.i. (Figure 3A). At 6 weeks p.i., 67% (6/9) of the mice developed GIN with dysplasia score above 3; three of them had submucosal invasive carcinoma (Figure 3B). At 10 weeks p.i., 4/9 mice developed GIN and two of them had submucosal invasive carcinoma (Figure 3C). The typhlocolitis was characterized by severely thickened mucosa, consisting of diffuse mucosal and submucosal inflammation, epithelia defects and edema, an abundance of hyperplasia and high grade dysplastic glands with submucosal invasion in polypoid adenomatous proliferation in the cecum (Figure 4). There was no gender difference with *H.japonicum*-induced inflammation in the ileo-cecal colic junction; but infected female mice had more severe lesions in the lower colon compared to infected male mice both at 6 and 10 weeks p.i. (Supplementary Figure 4, available at *Carcinogenesis* Online). *Helicobacter japonicum* induced multifocal hepatitis in infected mice at 6 weeks p.i. ($P < 0.05$), but there was no significant difference in hepatitis indexes at 10 weeks p.i between infected mice and control mice (Supplementary Figure 5,

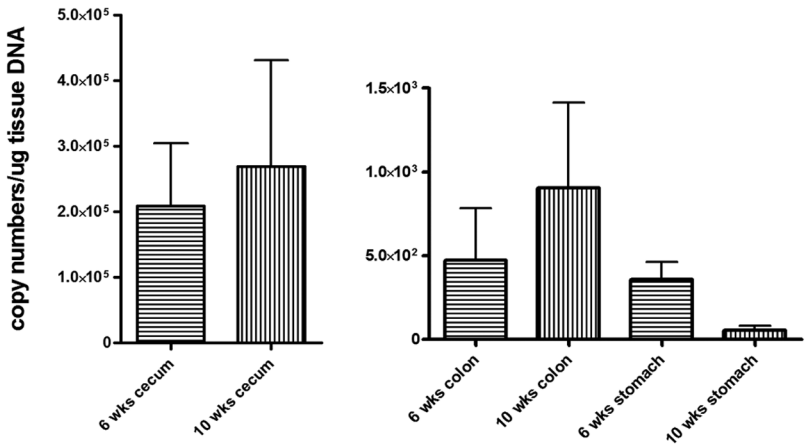

Figure 2. *Helicobacter japonicum* colonization in the stomach, colon and cecum of infected IL-10$^{-/-}$ mice. Quantitative PCR analysis with *Helicobacter* genus primers: All the infected mice had helicobacter colonization in the cecum and colon samples at both time points. The cecum had the highest colonization levels. There was no difference in the colonization levels between 6 and 10 weeks p.i.

available at *Carcinogenesis* Online). There were no significant lesions noticed in the stomach of helicobacter infected mice. All the control mice were clinically normal and no significant lesions were observed in their gastrointestinal tracts at 6 and 10 weeks p.i. No significant pathological lesions were observed in the control and infected C57BL/6 mice, but the background inflammation scores in the infected group were significantly higher (0.5) when compared to the control group ($P < 0.05$) (data not shown).

Helicobacter japonicum, MIT 01-6451, infection upregulated proinflammatory cytokine responses and iNOS mRNA levels in IL10$^{-/-}$ mice

Helicobacter japonicum infection in IL10$^{-/-}$ mice developed Th1-mediated typhlocolitis, previously reported in other EHS induced IBD in IL10$^{-/-}$ mouse models. In IL10$^{-/-}$ mice infected with *H.japonicum*, the most elevated cytokine was IL17a. At 6 weeks p.i., IL17a expression level in the cecum of infected mice was 500 times higher when compared with that of control cecum. At 10 weeks p.i, the IL17a level in infected mice was lower than 6 weeks p.i; but still 80 times higher than control mice ($P < 0.001$). Th1 cytokines INF-γ, TNF-α and iNOS expression levels were significantly elevated in infected mice as well, both at 6 and 10 weeks p.i. ($P < 0.01$). There were no changes on the gene expression levels of TH2 cytokines IL4 and IL6, as well as cytokine IL23a at 6 and 10 weeks p.i. (Figure 5A).

Seven cecum cytokine expressions were analyzed in C57BL/6 mice, and there were no changes in the IL4, IL6, IL23, TNFα and IFNγ expressions. Although IL17a and iNOS expression in C57BL mice were significantly increased in the infected group when compared to the control group, the magnitude levels in C57BL mice were much lower than the levels in IL10$^{-/-}$ mice (21 times less in IL17a expression and 5 times less in iNOS expression) (Supplementary Figure 6B, available at *Carcinogenesis* Online).

Helicobacter japonicum infection caused DNA double-strand breaks (DSB) in the intestinal tissues of infected mice

Double-stranded breaks are defined as DNA damage in which two complementary strands of double helix of DNA are damaged simultaneously in a location close to each other. It is considered to be the most dangerous type of DNA damage, and a single unrepaired DSB is sufficient for the induction of cell death. DSB can be initiated in response to a variety of stress signals that are encountered during physiological processes. When cells are exposed to ionizing radiation or DNA-damaging chemotherapeutic agents, DSBs are generated that rapidly result in the phosphorylation of histone H2A variant H2AX. Because phosphorylation of H2AX at Ser 139 (γ-H2AX) correlates well with each DSB, it is the most sensitive marker that can be used to examine the DNA damage produced and the subsequent repair of the DNA lesion (30,31). We used immunofluorescence staining γ-H2AX to detect DSB in the event of *H.japonicum* infection. There were considerable amounts of gut epithelial cells expressing positively for the gamma H2AX marker in the infected tissue, particularly within the tissues with histopathological changes of intestinal hyperplasia and dysplasia. In contrast, the uninfected tissue had very few cells which stained positively for gamma H2AX, suggesting there was little DNA damage to the intestinal epithelia without inflammation (Figure 5B). Cell proliferation in the ceca of IL10$^{-/-}$ mice were also evaluated by staining for Ki-67, a marker of cell proliferation; the frequency of Ki-67 positive cells was significantly increased in the ceca of infected mice (Figure 5C).

Discussion

Enterohepatic *Helicobacter* spp. (EHS) infections are endemic in many mouse colonies used in biomedical research. It has been reported that 88% of academic institutions worldwide were PCR-positive for EHS (10). Although EHS generally cause subclinical infection in immunocompetent mice, these infections can induce intestinal and hepatic tumors and have the potential to confound experimental data in mouse models (1,2,5,7,9,21,22). Coinfection of EHS and *H.pylori* either attenuated or promoted the severity of *H.pylori*-induced gastric pathology in C57BL/129 mice (32,33). In addition, EHS-induced inflammatory responses can alter host immune responses to unrelated specific experimental infections (1). We first isolated a novel *Helicobacter* sp. from mice shipped to our institute from Japan in 2001 (10). In this study, six more strains were isolated from mice obtained from additional Japanese research institutes allowing further characterization of this *Helicobacter* sp., which we have named *H.japonicum*.

Helicobacter japonicum is primarily isolated from mouse colonies in Asia. In the 2007 study by Taylor *et al.* (10), which surveyed helicobacter prevalence in mice originating from several countries, *H.japonicum* was only detected from mice

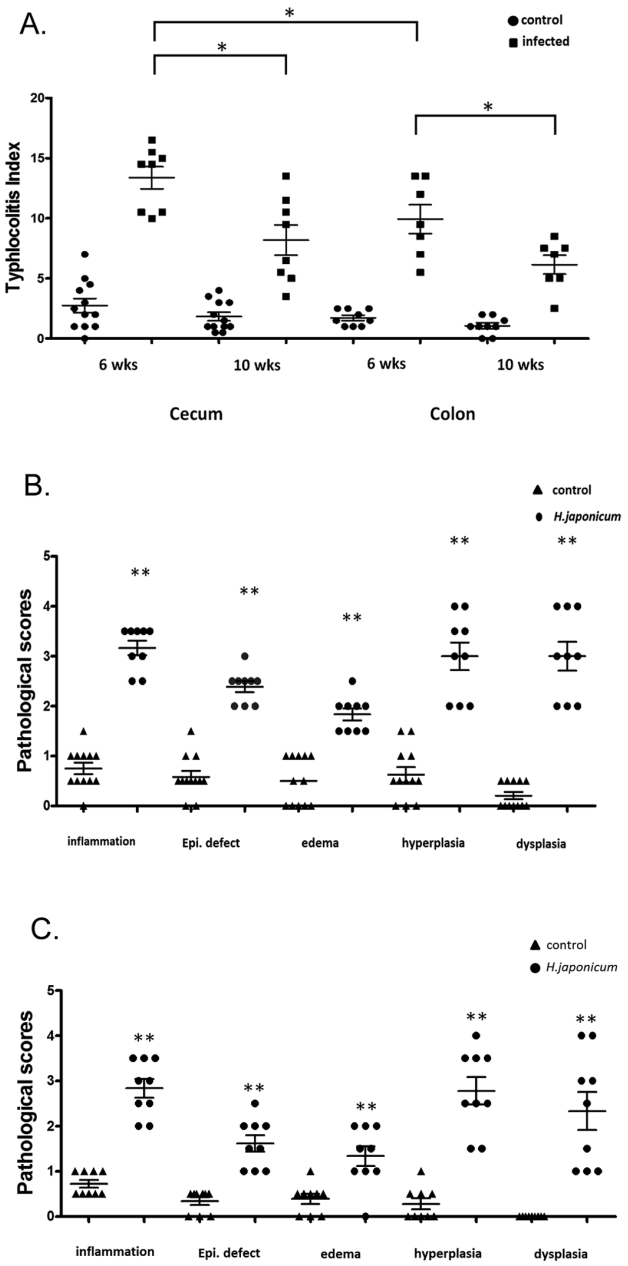

Figure 3. (**A**) *Helicobacter japonicum*-induced typlocolitis in IL10$^{-/-}$ mice. All the infected mice developed typhlocolitis at 6 weeks p.i. The typhlocolitis index in the colon and cecum of infected mice was significantly higher than that of control mice ($P < 0.01$). The cecum had more severe lesions than those observed in the colon. The lesions in the cecum at 6 weeks p.i were more severe than the cecum lesions at 10 weeks p.i. (* $P < 0.05$). (**B**) Cecum pathological scores of IL10$^{-/-}$ mice at 6 weeks p.i.: 67% (6/9) of the mice developed GIN with dysplasia score above 3; three of them had submucosal invasive carcinoma (**$P < 0.001$). (**C**) Cecum pathological scores of IL10$^{-/-}$ mice at 10 weeks p.i.: 4/9 mice developed GIN and two of them had submucosal invasive carcinoma (**$P < 0.001$).

obtained from research institutions in Japan, but not in mice from Europe or North America. In 2013, mouse colonies maintained in commercial and academic institutes in Japan were surveyed and found that a novel *Helicobacter* sp. that we now name *H.japonicum* had the highest prevalence among the *Helicobacter* spp. detected; however, the bacteria were not isolated from mice imported from Europe and the USA (12,34). It has also been reported that a novel *Helicobacter* sp., we have now named *H.japonicum*, is present at high frequency in laboratory mice in Thailand (35). In a previous report, *H.japonicum* was abundantly detected in the colon and cecum of clinically normal mice, while lower amounts were present in the stomach, gallbladder and other regions of the intestinal tract (12). The lack of clinical signs in these mice is consistent with our analysis of *H.japonicum*-infected C57BL mice or C57BL mice infected with *H.hepaticus*, which also did not have clinical signs (8,12). Importantly, however, it has been reported that the severe combined immunodeficient mice infected with *H.japonicum* had lower birth rates when compared with *Helicobacter* spp. free severe combined immunodeficient mice (36).

To study the pathogenic potential of *H.japonicum*, we infected IL10$^{-/-}$ mice with *H.japonicum* by oral gavage and necropsied the mice at 6 and 10 weeks p.i. *Helicobacter japonicum* successfully colonized the gastrointestinal tracts of all infected mice with the cecum being the primary colonization niche. *Helicobacter japonicum* was re-isolated from both the stomach and intestine, but was not detected in the liver. Infected animals had significant body weight loss and reduced activity at 10 weeks p.i; which resulted in an earlier necropsy date, 2 weeks ahead of schedule. Infected mice developed severe typhlocolitis by 6 weeks p.i, characterized by severely thickened mucosa with inflammation, high degree of hyperplasia and dysplasia as well as submucosal invasion in polypoid adenomatous proliferation in the ileo-cecal colic junction (Figure 4). The cumulative scoring of lesions in this region at 6 weeks p.i were more severe than the lesions at 10 weeks p.i. (Figure 3). This difference in pathology scores may be accounted for by one cage of five female mice, which were euthanized because of poor body scores prior to the designated necropsy time point. *Helicobacter japonicum*-induced typhlocolitis had similar pathological characteristics as other EHS induced IBD, such as *H.hepaticus*, *H.bilis*, *H.cinaedi* and *H.trogontum* in the IL10$^{-/-}$ mouse model. However, noteworthy was the finding that *H.japonicum* caused severe dysplasia as early as 6 week p.i. and 67% of the infected mice developed GIN with dysplasia score above 3. There were no correlations with helicobacter colonization levels and the severity of pathology in *H.japonicum* infected IL10$^{-/-}$ mice which is consistent with other EHS-induced intestinal disease in mouse models (22,25).

The pathological changes were more severe in the ileo-cecal colic junction of infected mice; however no gender difference was noted in this region of the bowel, but infected female mice had more severe lesions in the lower colon compared to infected male mice both at 6 and 10 weeks p.i. Genders play a critical role in helicobacter induced gastrointestinal diseases in mouse models. *Helicobacter hepaticus*-infected female A/J mice develop more severe intestinal inflammation and have significantly higher TH1 cytokine gene expression than infected males (37). *Helicobacter hepaticus*-infected C57BL/6 interleukin-10-deficient animals, male mice with *H.hepaticus* infection had more severe colitis as determined by histology and elevated levels of inflammatory cytokines in the colon at 6 weeks p.i (38). In our study, there were no differences in the cecum typhlocolitis index scores between genders, but the female mice had significantly higher pathological scores in the colon at both 6 and 10 weeks p.i. The underlying differences in the expression of cytokine receptors in different anatomical locations of the intestine may contribute to this difference (39).

At 6 weeks p.i, multifocal hepatitis was noticed in the infected mice which may indicate *H.japonicum* infection in the liver by translocating the intestinal barrier into hepatic tissues or alternatively, indirect effect of systemic cytokine response due to the primary intestinal infection (40). Even though we did not detect *H.japonicum* in the liver samples, in another study *H.japonicum*

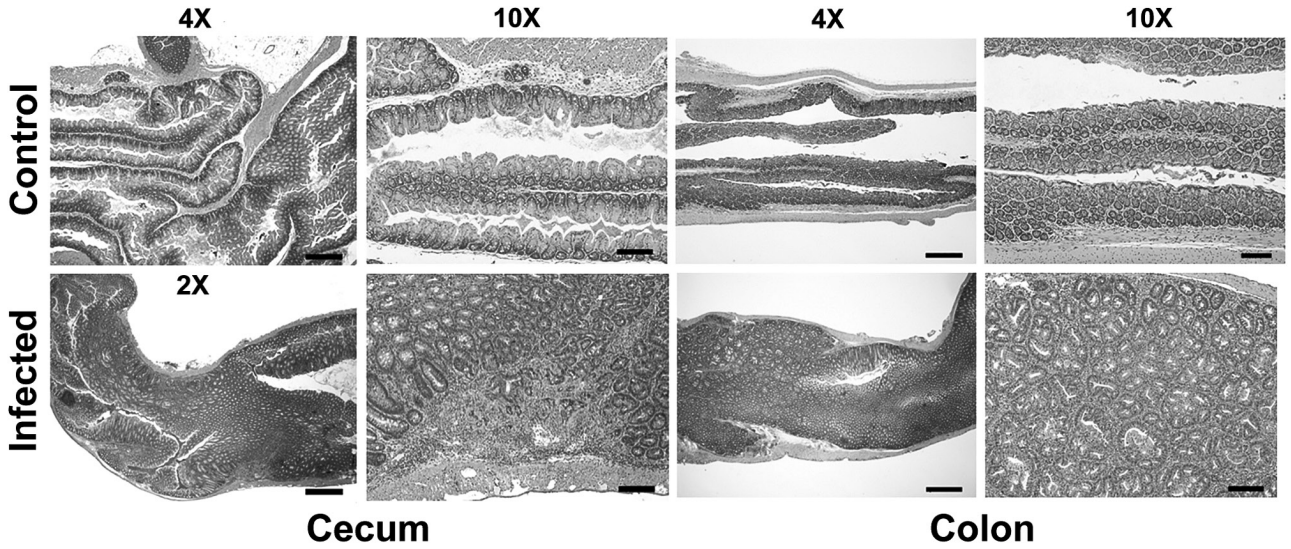

Figure 4. Representative hematoxylin and eosin (H&E) images of the colon and cecum of IL10$^{-/-}$ mice at 6 weeks p.i. At 6 weeks p.i., infected mice have severely thickened mucosa, consisting of diffuse mucosal and submucosal inflammation, an abundance of hyperplastic and high grade dysplastic glands with submucosal invasion in the cecum. (2× bar = 800 μm; 4× bar = 400 μm; 10× bar = 150 μm).

was identified in 33% gallbladder samples tested; however, they too did not detect the organism in liver samples (12).

Helicobacter infections develop a Th1/Th17-associated typholocolitis in mice with IL-10 impaired signaling. *Helicobacter hepaticus* infection gave rise to TH17 cells that induced IL17A secretion and elicited IFN-γ induction; both of which contributed to intestinal pathology (41). It also has been suggested recently that IL-17A can trigger gastrointestinal tumor development (42). Innate and adaptive immune responses responsible for IL17 production have carcinogenic potential, promoting tumor initiation and growth (43). Furthermore, the presence of IL-17A-producing cells in patients is associated with a poor prognosis for both gastric (44) and colorectal cancers (45). IL17 producing TH17 cells have been shown to promote carcinogenesis in many tumor tissues, including microbe-driven colon cancer (43). In our study, TIL17a was the most significantly elevated cytokine both at 6 and 10 weeks p.i.; 33 and 22% of the mice developed submucosal invasive carcinoma, respectively, at these two time points p.i.

Helicobacter japonicum contains CDT genes. CDT is produced by many EHS and is considered a virulence factor. *Helicobacter japonicum* CDT caused cell cycle arrest in Hela S3 cells (data not show). CDT of *H.hepaticus* and *H.pullorum* induced a TH17 related response and an antimicrobial signature in intestinal and hepatic cells in vitro (46). *Helicobacter hepaticus* induced a CDT-dependent proinflammatory cytokine IL8 induction in human epithelial cells, activation of NF-kB pathway, and TH1 and TH17-related inflammation associated genes and genes encoding antimicrobial products by microarray analysis. Those genes are known to play a role in cancer. In the *H.hepaticus*-induced hepatocellular carcinoma model, the presence of CDT enhances expression of a proinflammatory cytokines such as TNF-α, IL-6 and COX-2, activates the NF-κB pathway and antiapoptotic Bcl-2 and Bcl-XL in the inflamed livers (47) which leads to increased expression of downstream growth mediators IL-6 and TGF-α compared with the CDT-negative mutant. The combination of these effects could be beneficial for cell survival in the early phase of the infection. The sustained overproduction of IL-6 and anti-apoptotic proteins Bcl-2 and Bcl-XL facilitates proliferation of the inflamed cells, thereby promoting the development of pre-malignant dysplastic lesions that ultimately give rise to cancer (47,48). In the ceca of *H.japonicum* infected mice, the γ-H2AX staining, the marker for DNA DSBs, was significantly increased when compared with control ceca. CDT has nuclease activity, causes DNA DSBs, inhibits ATM-dependent response pathways and suppresses repair of DNA adducts. Importantly, *H.hepaticus* infection in 129 rag deficient mice cause inflammatory immune responses associated with highly reactive oxygen and nitrogen species capable of causing tissue injury, death or mutation of cells (49–51). Further, DSBs have been involved with *H.pylori*-induced gastric cancer (52).

In *H.japonicum*-infected IL10$^{-/-}$ mice, iNOS was overexpressed in the inflamed intestine. The significantly increased Ki-67 staining in the cecum of infected Il10$^{-/-}$ mice indicated the presence of overlapping inflammation and cell proliferation in *H.japonicum* infected mice causing cell damage, DSBs, presumably DNA mutations, resulting in genomic instability and enhanced risk of carcinogenesis. This model provides an ideal *in vivo* system to study the etiopathogenesis of lower bowerl carcinoma.

Description of *Helicobacter japonicum* sp. nov.

Helicobacter japonicum [*japonicum* N.L. gen. masc. n. of Japan; where the bacterium was first isolated from mice imported from Japan].

The organism is motile; cells are slender, slightly curved rods (2–3μm) with single sheathed polar flagellum. The bacterium is Gram-negative and non-sporulating. The organism grows slowly and appears on solid agar as a spreading film on the surface. The bacterium grows at 37°C and 42°C, but not at 25°C, under microaerobic conditions, but not aerobically. The bacterium is oxidase and catalase positive, but urease, alkaline phosphatase, indoxyl acetate hydrolysis and nitrate reduction are negative. It does not grow on 1% glycine and is resistant to cephalothin and nalidixic acid. The type strain MIT 01-6451T, has been deposited in the BCCM/LMG Bacteria Collection as LMG 28612. It has a DNA G+C content of 37.5%, and its genome is 2 Mb.

The draft genome of MIT 01-6451 has been submitted to Genbank under accession number JRMQ00000000.

Supplementary material

Supplementary Tables 1 and 2 and Figure 1–6 can be found at http://carcin.oxfordjournals.org/

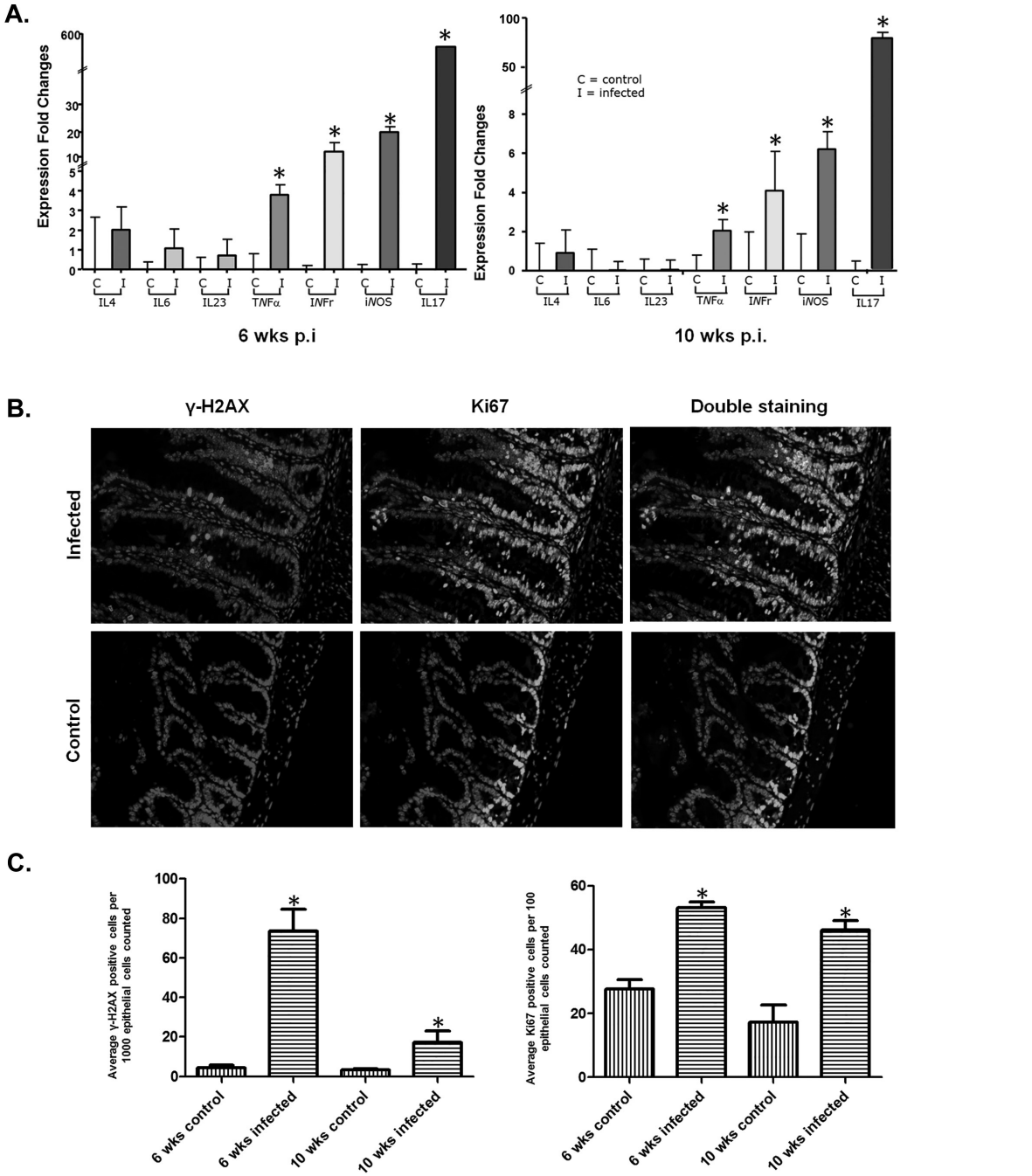

Figure 5. (**A**) Cecum cytokine mRNA profiles of *H.japonicum* infected IL10$^{-/-}$ mice (*$P < 0.01$). (**B**) Immunofluorescence staining of IL10$^{-/-}$ mice cecum for γ-H2AX (in red), Ki67 (in green) and cell nuclei (in blue); large amount of gut epithelial cells stained positively in the infected tissue, particularly within regions of intestinal hyperplasia and dysplasia; the uninfected tissue had very few cells stained positively for both markers; (B) *$P < 0.01$. (**C**) Average γ-H2AX positive cells per 1000 (left) and 100 (right) epithelial cells counted. *$P < 0.01$.

Funding

National Institutes of Health (P30-ES002109, R01-OD01141, T32-OD010978 all to J.G.F).

Acknowledgements

We thank Hans Tuper for providing taxonomic expertise in naming of this novel *Helicobacter* sp., and Alyssa Pappa for assistance with manuscript preparation.

Conflict of Interest Statement: None declared.

References

1. Fox, J.G. et al. (2011) *Helicobacter hepaticus* infection in mice: models for understanding lower bowel inflammation and cancer. Mucosal Immunol., 4, 22–30.
2. Nguyen, D.D. et al. (2013) Colitis and colon cancer in WASP-deficient mice require helicobacter species. Inflamm. Bowel Dis., 19, 2041–2050.
3. Fox, J.G. et al. (1995) *Helicobacter bilis* sp. nov., a novel Helicobacter species isolated from bile, livers, and intestines of aged, inbred mice. J. Clin. Microbiol., 33, 445–454.
4. Franklin, C.L. et al. (1998) Enterohepatic lesions in SCID mice infected with *Helicobacter bilis*. Lab. Anim. Sci., 48, 334–339.

5. Maggio-Price, L. et al. (2002) *Helicobacter bilis* infection accelerates and *H. hepaticus* infection delays the development of colitis in multiple drug resistance-deficient (mdr1a-/-) mice. Am. J. Pathol., 160, 739–751.
6. Maurer, K.J. et al. (2005) Identification of cholelithogenic enterohepatic helicobacter species and their role in murine cholesterol gallstone formation. Gastroenterology, 128, 1023–1033.
7. Hailey, J.R. et al. (1998) Impact of *Helicobacter hepaticus* infection in B6C3F1 mice from twelve National Toxicology Program two-year carcinogenesis studies. Toxicol. Pathol., 26, 602–611.
8. Whary, M.T. et al. (2001) Long-term colonization levels of *Helicobacter hepaticus* in the cecum of hepatitis-prone A/JCr mice are significantly lower than those in hepatitis-resistant C57BL/6 mice. Comp. Med., 51, 413–417.
9. Fox, J.G. et al. (2004) Helicobacter bilis-associated hepatitis in outbred mice. Comp. Med., 54, 571–577.
10. Taylor, N.S. et al. (2007) Enterohepatic Helicobacter species are prevalent in mice from commercial and academic institutions in Asia, Europe, and North America. J. Clin. Microbiol., 45, 2166–2172.
11. Hayashimoto, N. et al. (2013) Current microbiological status of laboratory mice and rats in experimental facilities in Japan. Exp. Anim., 62, 41–48.
12. Yamanaka, H. et al. (2013) Prevalence of an unidentified Helicobacter species in laboratory mice and its distribution in the hepatobiliary system and gastrointestinal tract. Exp. Anim., 62, 109–116.
13. Hirota, T. et al. (2011) Drug-inducible gene recombination by the Dppa3-MER Cre MER transgene in the developmental cycle of the germ cell lineage in mice. Biol. Reprod., 85, 367–377.
14. Hanno, Y. et al. (2003) Tracking mouse visual pathways with WGA transgene. Eur. J. Neurosci., 18, 2910–2914.
15. Meno, C. et al. (1998) lefty-1 is required for left-right determination as a regulator of lefty-2 and nodal. Cell, 94, 287–297.
16. Kaur, T. et al. (2011) *Campylobacter troglodytis* sp. nov., isolated from feces of human-habituated wild chimpanzees (Pan troglodytes schweinfurthii) in Tanzania. Appl. Environ. Microbiol., 77, 2366–2373.
17. Sheh, A. et al. (2013) Phylogeographic origin of *Helicobacter pylori* determines host-adaptive responses upon coculture with gastric epithelial cells. Infect. Immun., 81, 2468–2477.
18. Zerbino, D.R. et al. (2008) Velvet: algorithms for de novo short read assembly using de Bruijn graphs. Genome Res., 18, 821–829.
19. Klimke, W. et al. (2009) The National Center for Biotechnology Information's Protein Clusters Database. Nucleic Acids Res., 37, D216–23.
20. Fox, J.G. et al. (1998) Hepatic Helicobacter species identified in bile and gallbladder tissue from Chileans with chronic cholecystitis. Gastroenterology, 114, 755–763.
21. Erdman, S.E. et al. (2003) CD4(+)CD25(+) regulatory lymphocytes require interleukin 10 to interrupt colon carcinogenesis in mice. Cancer Res., 63, 6042–6050.
22. Erdman, S.E. et al. (2009) Nitric oxide and TNF-alpha trigger colonic inflammation and carcinogenesis in *Helicobacter hepaticus*-infected, Rag2-deficient mice. Proc. Natl. Acad. Sci. USA, 106, 1027–1032.
23. Huijsdens, X.W. et al. (2004) Detection of Helicobacter species DNA by quantitative PCR in the gastrointestinal tract of healthy individuals and of patients with inflammatory bowel disease. FEMS Immunol. Med. Microbiol., 41, 79–84.
24. Ge, Z. et al. (2001) Fluorogenic PCR-based quantitative detection of a murine pathogen, Helicobacter hepaticus. J. Clin. Microbiol., 39, 2598–2602.
25. Shen, Z. et al. (2015) *Helicobacter cinaedi* induced typhlocolitis in Rag-2-deficient mice. Helicobacter, 20, 146–155.
26. Chan, V. et al. (2005) Visualization of Helicobacter species within the murine cecal mucosa using specific fluorescence in situ hybridization. Helicobacter, 10, 114–124.
27. Sheh, A. et al. (2014) Draft genome sequences of eight enterohepatic helicobacter species isolated from both laboratory and wild rodents. Genome Announ., 2, e01218–14.
28. Bartonickova, L. et al. (2013) Hcp and VgrG1 are secreted components of the *Helicobacter hepaticus* type VI secretion system and VgrG1 increases the bacterial colitogenic potential. Cell. Microbiol., 15, 992–1011.
29. Maurer, K.J. et al. (2006) *Helicobacter pylori* and cholesterol gallstone formation in C57L/J mice: a prospective study. Am. J. Physiol. Gastrointest. Liver Physiol., 290, G175–G182.
30. Turinetto, V. et al. (2015) Multiple facets of histone variant H2AX: a DNA double-strand-break marker with several biological functions. Nucleic Acids Res., 43, 2489–2498.
31. Ivashkevich, A. et al. (2012) Use of the γ-H2AX assay to monitor DNA damage and repair in translational cancer research. Cancer Lett., 327, 123–133.
32. Ge, Z. et al. (2011) Coinfection with Enterohepatic Helicobacter species can ameliorate or promote *Helicobacter pylori*-induced gastric pathology in C57BL/6 mice. Infect. Immun., 79, 3861–3871.
33. Lemke, L.B. et al. (2009) Concurrent *Helicobacter bilis* infection in C57BL/6 mice attenuates proinflammatory *H. pylori*-induced gastric pathology. Infect. Immun., 77, 2147–2158.
34. Goto, K. et al. (2000) Current status of Helicobacter contamination of laboratory mice, rats, gerbils, and house musk shrews in Japan. Curr. Microbiol., 41, 161–166.
35. Duangchanchot, M. et al. (2014) Prevalence of helicobacter in laboratory mice in Thailand. Exp. Anim., 63, 169–173.
36. Yamanaka, H. et al. (2015) Helicobacter sp. MIT 01-6451 infection during fetal and neonatal life in laboratory mice. Exp. Anim., 64, 375–382.
37. Livingston, R.S. et al. (2004) Sex influence on chronic intestinal inflammation in *Helicobacter hepaticus*-infected A/JCr mice. Comp. Med., 54, 301–308.
38. Irwin, R. et al. (2013) Colitis-induced bone loss is gender dependent and associated with increased inflammation. Inflamm. Bowel Dis., 19, 1586–1597.
39. Morrison, P.J. et al. (2015) Differential requirements for IL-17A and IL-22 in cecal versus colonic inflammation induced by *Helicobacter hepaticus*. Am. J. Pathol., 185, 3290–3303.
40. Fox, J.G. et al. (2010) Gut microbes define liver cancer risk in mice exposed to chemical and viral transgenic hepatocarcinogens. Gut, 59, 88–97.
41. Morrison, P.J. et al. (2013) Th17-cell plasticity in *Helicobacter hepaticus*-induced intestinal inflammation. Mucosal Immunol., 6, 1143–1156.
42. Ericksen, R.E. et al. (2014) Obesity accelerates *Helicobacter felis*-induced gastric carcinogenesis by enhancing immature myeloid cell trafficking and TH17 response. Gut, 63, 385–394.
43. Housseau, F. et al. (2016) Redundant innate and adaptive sources of IL-17 production drive colon tumorigenesis. Cancer Res. , 76, 2115–2124.
44. Zhuang, Y. et al. (2012) CD8(+) T cells that produce interleukin-17 regulate myeloid-derived suppressor cells and are associated with survival time of patients with gastric cancer. Gastroenterology, 143, 951–62.e8.
45. Tosolini, M. et al. (2011) Clinical impact of different classes of infiltrating T cytotoxic and helper cells (Th1, th2, treg, th17) in patients with colorectal cancer. Cancer Res., 71, 1263–1271.
46. Péré-Védrenne, C. et al. (2016) The cytolethal distending toxin subunit CdtB of Helicobacter induces a Th17-related and antimicrobial signature in intestinal and hepatic cells *in vitro*. J. Infect. Dis., 213, 1979–1989.
47. Ge, Z. et al. (2007) Bacterial cytolethal distending toxin promotes the development of dysplasia in a model of microbially induced hepatocarcinogenesis. Cell Microbiol., 9, 2070–2080.
48. Rogers, A.B. et al. (2004) Inflammation and cancer. I. Rodent models of infectious gastrointestinal and liver cancer. Am. J. Physiol. Gastrointest. Liver Physiol., 286, G361–G366.
49. Wogan, G.N. et al. (2012) Infection, inflammation and colon carcinogenesis. Oncotarget, 3, 737–738.
50. Mangerich, A. et al. (2012) Infection-induced colitis in mice causes dynamic and tissue-specific changes in stress response and DNA damage leading to colon cancer. Proc. Natl. Acad. Sci. USA, 109, E1820–E1829.
51. Knutson, C.G. et al. (2013) Chemical and cytokine features of innate immunity characterize serum and tissue profiles in inflammatory bowel disease. Proc. Natl. Acad. Sci. USA, 110, E2332–E2341.
52. Toller, I.M. et al. (2011) Carcinogenic bacterial pathogen Helicobacter pylori triggers DNA double-strand breaks and a DNA damage response in its host cells. Proc. Natl. Acad. Sci. USA, 108, 14944–14949.